Journal of Aerosol Science 157 (2021) 105818

Contents lists available at ScienceDirect

Journal of Aerosol Science

journal homepage: www.elsevier.com/locate/jaerosci

Calibration of optical particle size spectrometers against a primary standard: Counting efficiency profile of the TSI Model 3330 OPS and Grimm 11-D monitor in the particle size range from 300 nm to 10 μm

Konstantina Vasilatou [a,*,1], Christian Wälchli [a,1], Stig Koust [b], Stefan Horender [a], Kenjiro Iida [c], Hiromu Sakurai [c], Friedhelm Schneider [d], Jürgen Spielvogel [e], Thomas Y. Wu [f], Kevin Auderset [a]

[a] Laboratory Particles and Aerosols, Federal Institute of Metrology METAS, 3003, Bern, Switzerland
[b] Environmental Technology, Danish Technological Institute (DTI), Aarhus, Denmark
[c] National Metrology Institute of Japan (NMIJ), National Institute of Advanced Industrial Science and Technology (AIST), 1-1-1 Umezono, Tsukuba, Ibaraki, Japan
[d] GRIMM Aerosol Technik Ainring GmbH & Co. KG, Ainring, Germany
[e] TSI GmbH, Neukölln Str. 4, 52068, Aachen, Germany
[f] National Metrology Center, Agency for Science, Technology and Research (A*STAR), 2 Fusionopolis Way, #08-05, Innovis, Singapore

ARTICLE INFO

Keywords:
Calibration
Optical particle size spectrometers
Counting efficiency
Polystyrene particles
Standardisation

ABSTRACT

In this study, we present a traceable method for determining the counting efficiency of optical particle size spectrometers (OPSS), also known as aerosol spectrometers. The primary standard consists of an aerosol generation setup, a vertical flow tube for particle homogenization and a reference optical particle counter. The OPSS under testing and the reference optical particle counter sample aerosol simultaneously through specially designed isokinetic sampling probes at number concentrations ranging from 0.5 cm^{-3} up to several hundred particles per cm^3 (depending on the particle size). Calibration in terms of particle size relies by convention on the use of certified PS (polystyrene) spheres in the size range 100 nm - 10 μm. Here, the counting efficiency profiles of two commonly used OPSS, namely the Model 3330 OPS (TSI Inc., USA) and the 11-D monitor (Grimm GmbH, Germany) are presented for the first time and discussed within the context of the ISO 21501–1:2009 and 21501–4:2018 standards on the calibration of OPSS for indoor/outdoor measurements and optical particle counters (OPC) for clean rooms applications, respectively. We believe that this study can help manufacturers improve the design of their instruments, contribute to the further development of relevant national and international standards and pave the way for a standardised and traceable calibration of OPSS units installed at air quality monitoring stations and industrial/workplace environments.

* Corresponding author.
E-mail address: Konstantina.Vasilatou@metas.ch (K. Vasilatou).
[1] These authors have contributed equally.

https://doi.org/10.1016/j.jaerosci.2021.105818
Received 22 March 2021; Received in revised form 3 May 2021; Accepted 4 May 2021
Available online 27 May 2021

1. Introduction

One of the most important metrics to describe the physical properties of the atmospheric aerosol and its impact on climate is the particle number size distribution (Mann et al., 2014). Several optical particle size spectrometers (OPSS, also known as light-scattering aerosol spectrometers LSAS or simply aerosol spectrometers) have been developed to monitor ambient particle size distributions starting from 100 nm − 300 nm (depending on the OPSS model) and going up to several micrometres. The wide measurement range, fast measurement time, compact size and lack of any hazardous material (e.g. radioactive sources) make them ideal for ground (Renard et al., 2016) as well as aircraft and balloon-borne measurements (Deshler, Hervig, Hofmann, Rosen, & Liley, 2003; Krejci et al., 2003; Ortega, Snider, Smith, & Reeves, 2019; Renard et al., 2016). Recently, OPSS are increasingly being used for workplace and indoor air quality monitoring (Bush, Heflin, Marek, Bryant, & Auvermann, 2014; Din et al., 2020; Maragkidou, Jaghbeir, Hämeri, & Hussein, 2018) and low-cost optical sensors are evaluated for use on-board unmanned aerial vehicles (Bezantakos, Schmidt-Ott, & Biskos, 2018).

To derive accurate size distributions, the OPSS detection efficiency must be determined in a traceable manner against a primary standard for particle number concentration. For size calibration, spherical non-absorbing PS (polystyrene) particles of known diameter and refractive index are typically used (ISO 21501-1, 2009; ISO 21501-4, 2018). Since ambient aerosols contain particles of different shapes, sizes and complex refractive index, the measured particle size distributions must be post-corrected by assuming a complex refractive index for the local ambient aerosol which was monitored (Alas et al., 2019; Hermann et al., 2016; Kim, 1995; Rosenberg et al., 2012). Alternatively, the method based on an aerodynamic aerosol classifier (AAC) (Sang-Nourpour & Olfert, 2019) and atmospheric particles as calibration particles can be used.

First attempts have been made within the ISO 21501–1:2009 document (ISO 21501-1, 2009) to standardise the first two steps, i.e. the determination of the counting efficiency and the size calibration with PS particles of certified size, but the ISO standard is still incomplete. For instance, it provides no information on the primary standard for number concentration nor does it define which size channels of the OPSS must be taken into account when determining the OPSS counting efficiency.

As a result, no standardised calibration procedures for OPSS exist to date. In a good number of field studies, the OPSS are used as received from factory without further calibration (Alas et al., 2019; Bezantakos et al., 2018) or the OPSS counting efficiency is evaluated based on Poisson counting statistics combined with uncertainties due to electronic noise and inlet sampling efficiency (Renard et al., 2016). In other cases, reference measurements with a scanning mobility particle sizer (SMPS) (Sousan, Koehler, Hallett, & Peters, 2016) or a calibrated condensation particle counter (CPC) (Hermann et al., 2016; Kupc, Williamson, Wagner, Richardson, & Brock, 2018; Sang-Nourpour & Olfert, 2019; Stolzenburg, Kreisberg, & Hering, 1998) are carried out in order to determine the OPSS counting efficiency. Using an SMPS or CPC as reference instrument, however, has the following limitations:

- Traceability for CPCs has been established through comparison with electrometers only for number concentrations above 1000 cm^{-3} (Högström et al., 2014). Below this limit, a proportionality assessment over the range of the CPC must be carried out (Owen, Mulholland, & Guthrie, 2012)
- The CPC detection efficiency decreases above 1 μm (Järvinen, Keskinen, & ; Yli-Ojanperä et al., 2012)
- In most cases, the CPC must be combined with a Differential Mobility Analyser (DMA) for upstream particle size classification. This method is only suited for sub-micrometre particles unless a large custom-made DMA column is used (Järvinen et al., 2018). By using an AAC, particles with an aerodynamic diameter of up to about 5 μm can be size-selected; however, care must be taken to apply the method only in the size range where the CPC counting efficiency is known (Tran et al., 2020).
- The aerosol inlet of the CPC is not located on the top of the instrument as in the case of the OPSS but on the side. The tubing connecting the aerosol generator and the CPC is therefore bent, and this may lead to considerable particle losses especially for particle sizes equal to or larger than 1 μm.

Moreover, methods relying on the use of a vibrating orifice aerosol generator (VOAG) for producing model aerosols in the micrometre range might be very useful for sizing studies (Chen, Cheng, & Yeh, 1984; Liu, Berglund, & Agarwal, 1974) but cannot serve as a number concentration standard since the VOAG often generates satellite droplets and almost always generates doublets which account for a few percent of the total particle number (Iida, Sakurai, Saito, & Ehara, 2014).

To overcome such limitations, two primary standards for particle number concentration have recently been reported. The first primary standard, developed at the Federal Institute of Metrology METAS (Switzerland), consists of an aerosol generation setup, a vertical flow tube for particle homogenization and a reference particle counter, and has already been applied in the calibration of CPC, OPC for cleanroom applications and bioaerosol monitors (Horender, Auderset, & Vasilatou, 2019; Sauvageat et al., 2020). This method relies on the use of certified PS spheres in the size range 100 nm - 10 μm and number concentration range from 0.5 cm^{-3} up to about 2000 cm^{-3} (depending on the particle size). The wide particle size and concentration range makes this method ideal for calibrating instruments designed for ambient aerosol monitoring.

The second primary standard, based on an inkjet aerosol generator (IAG), was developed at the National Institute of Advanced Industrial Science and Technology (AIST, Japan) (Iida et al., 2014; Iida & Sakurai, 2018). IAG generates particles at a known and constant rate, thus eliminating the need for a reference counter. The method is well suited for generating particles made of water-soluble material such as lactose monohydrate and ionic liquid with aerodynamic and volume equivalent diameters up to 10 μm. However, the smallest particle size that can be generated is limited by the size of the residue particles arising from solvent (water) impurities. In practice, generating particles with d_{PS} (i.e. diameter of PS spheres with light-scattering intensity equal to that of a given test particle) below 500 nm can be challenging (Iida et al., 2014; Iida & Sakurai, 2018). Moreover, the number concentrations

generated by the IAG are typically below 1 cm^{-3}. Nevertheless, the measurement uncertainties remain small even at such low concentrations since a tested OPC directly counts the particles generated by the IAG; therefore, the uncertainty of particle counts does not have a random component due to Poisson sampling process.

To the best of our knowledge, no primary method for the calibration of OPSS in the micrometre range and at atmospherically relevant concentrations has been demonstrated to date. The purpose of this study is threefold: i) to demonstrate how the METAS primary standard can be applied in the calibration of OPSS, ii) to present, for the first time, the counting efficiency profiles of two commonly used OPSS, namely the Model 3330 OPS (TSI Inc., USA) and the 11-D monitor (Grimm GmbH, Germany) for sizes up to 10 μm, and iii) to make recommendations for the further development of the ISO 21501–1:2009 standard.

2. Material and methods

2.1. Primary standard for particle number concentration at METAS

The custom-made experimental facility at METAS for the calibration of OPSS is a further development of the facility for the calibration of OPC (optical particle counters) for cleanroom applications described in (Horender et al., 2019). Only the main aspects will be discussed here with emphasis on the components which have been modified for the work reported in this paper.

As illustrated in Fig. 1, the experimental set up consists of three distinct sections: the aerosol generation system (upper right section, three different aerosol generation paths are shown), a turbulent flow tube (homogenizer) and the particle detection system. PS aerosols

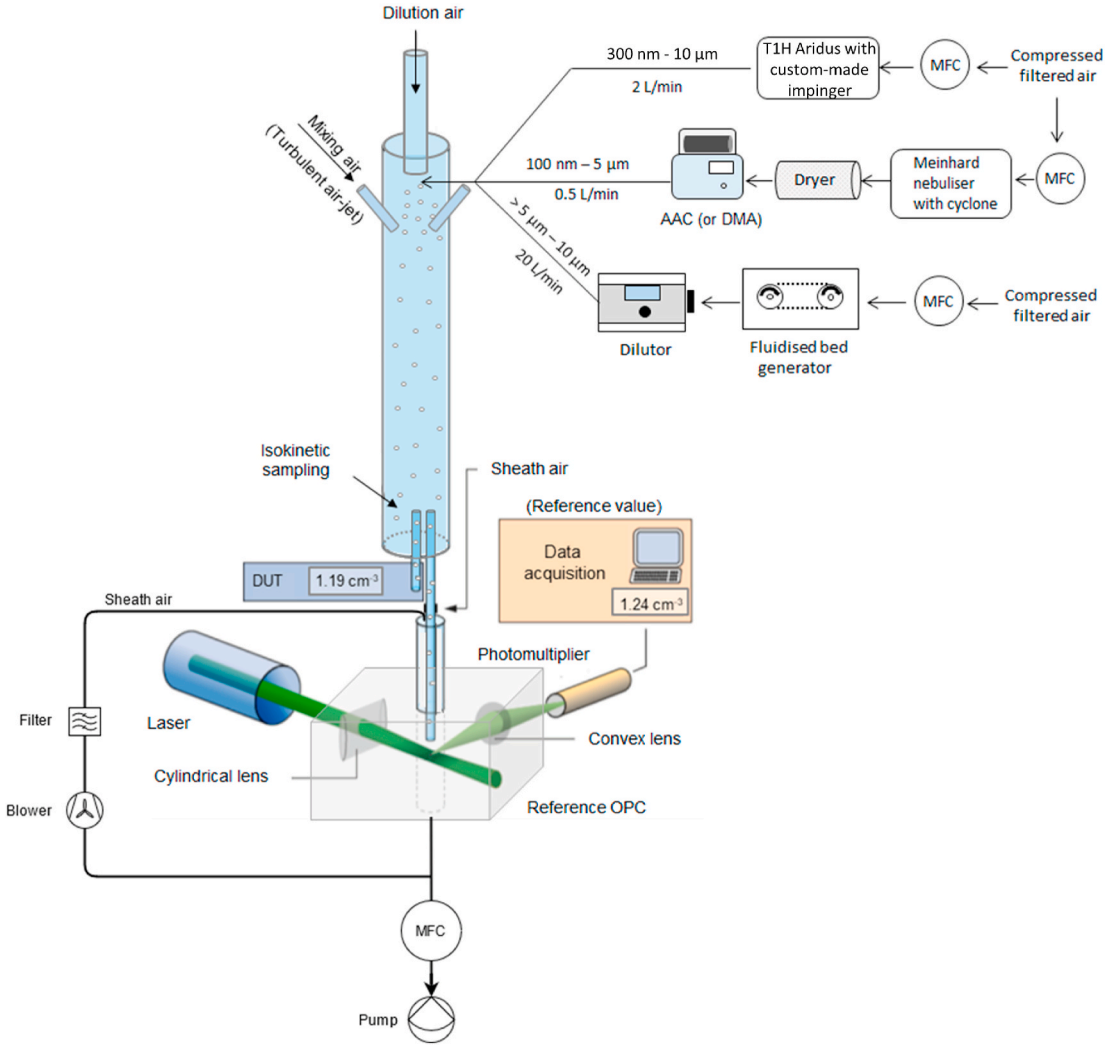

Fig. 1. Schematic representation (simplified) of the experimental facility at METAS. For a more detailed description of the set-up the readers are referred to Horender et al. (Horender et al., 2019). DUT, MFC and AAC stand for device under test, mass flow controller and aerodynamic aerosol classifier, respectively. The design of the isokinetic sampling probes is displayed in Fig. 3.

in the size range 100 nm - 10 μm are generated based on wet or dry dispersion using commercially available generators (Horender et al., 2019), and depending on the specific application, they can be size-selected by an AAC or differential mobility analyser (DMA) to filter out residue particles. Whenever high particle number concentrations are required, the use of the AAC is preferable due to the higher particle transmission efficiency (Johnson, Irwin, Symonds, Olfert, & Boies, 2018). In this study, PS particles with diameter up to 1 μm were generated with the Meinhard nebuliser while particles in the size range 2 − 10 μm with a model T1H ARIDUS nebuliser (Teledyne CETAC Technologies, USA), equipped with a custom-made impinger. Particles with a diameter of 10 μm (or larger) can also be dispersed from dry powder by a fluidised bed generator as shown in Fig. 1.

Care must be taken when aerosolising PS suspensions at high concentrations since PS dimers can be formed. In Fig. 2, the normalised counts of the reference optical particle counter are plotted as a function of the channel number when nebulising an aqueous suspension of 1 μm PS particles with the Meinhard generator. Apart from the main peak of PS monomers at channel numbers 300–380, a broad peak due to residue particles arising from additives in the PS suspension (channel numbers 100–250) and a narrow peak of PS dimers (channel numbers 370–400) are observed. In this example, by using an AAC for particle size selection, the residual particles and PS dimers could be filtered out (see red trace of Fig. 2).

The homogenizer is a 4-m-long custom-made stainless-steel tube with an inner diameter of 16.4 cm, oriented vertically. Dry filtered air at a fixed flow rate of 120 L/min enters the homogenizer from the very top and sweeps the PS particles down the tube, where they are further mixed by three turbulent air-jets. The air-jet injection tubes are placed symmetrically around the homogenizer tube pointing 60° downwards. Each turbulent air jet has a flow rate of 20 L/min. The sampling zone is located 3.0 m downstream of the injection position and accommodates two isokinetic sample probes, one for the reference optical particle counter and one for the device under test (DUT), which are placed just above the outlet of the homogenizer.

The detection system consists of a custom-built optical particle counter placed right at the outlet of the homogenizer to minimize particle losses in the connection tubes. The sampled aerosol enters the detection chamber through a nozzle with an orifice of 0.2 mm and is surrounded by a sheath-air flow, which prevents the particle beam from diverging. The sampling flow is measured with a traceably calibrated mass flow meter and is set to ≤60 mL/min to avoid any coincidence losses. To confirm that no coincidence losses occur, a comparison with a CPC (traceably calibrated according to ISO 27891 (ISO-27891, 2015)) using PS particles of 200 nm–300 nm is carried out before each calibration campaign (see section S1 in the Supporting Information). A laser beam is generated by a continuous-wave laser (5 Watt, Verdi V-5, Coherent, USA) at a wavelength of 532 nm, and focused at the point of intersection with the aerosol stream with the use of a cylindrical lens. Particles crossing the laser sheet (width of 0.7 mm) scatter light, which is detected by a photomultiplier tube placed at a 90° angle.

Since the aerosol inlet flow rate of the OPSS for ambient air measurements is typically in the range 1–5 L/min, as opposed to the much higher sampling flow rate of OPC for cleanroom monitoring, a new set of isokinetic sampling probes was designed. As an example, the design of the isokinetic sampling probe for an OPSS with flow rate of 0.1 ft^3/min (=2.83 L/min) is shown in Fig. 3a) and b) (left probe). For comparison, the design of the isokinetic sampling probe for an OPC with flow rate of 28.3 L/min (=1 ft^3/min) is displayed in Fig. 3a) and b) (right probe). All isokinetic sampling probes are made of aluminium.

All mass flow controllers used in the aerosol generation or detection parts of the setup are calibrated at METAS in a traceable manner (0.30% relative expanded uncertainty). The counter and peak-detection algorithm of the reference particle counter have been calibrated with respect to the national standard of frequency by generating pulses of known frequency, duration and line shape (single and double peaks). For a more detailed discussion on measurement traceability the readers are referred to (Horender et al., 2019).

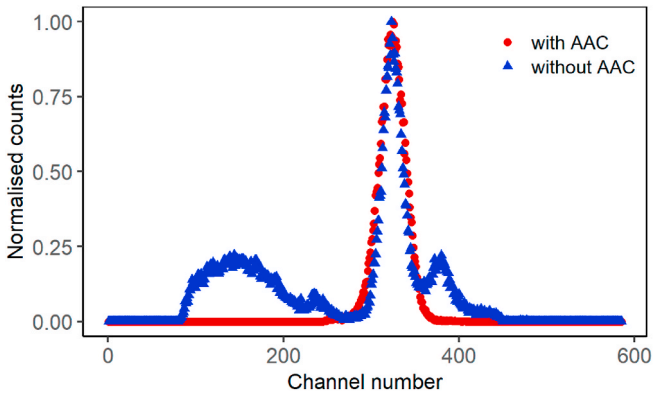

Fig. 2. Normalised counts measured by the reference optical particle counter as a function of the channel number when nebulising an aqueous suspension of 1 μm PS particles with the Meinhard generator. The blue trace was recorded without size selecting the particles with an AAC. The first broad peak at channel numbers 100–250 corresponds to residue particles, the second (main) peak to PS monomers (1 μm) and the weak overlapping peak at channel numbers 370–400 to PS dimers. The red trace was recorded with an AAC downstream of the nebuliser which selected the peak corresponding to the PS monomers. (For interpretation of the references to colour in this figure legend, the reader is referred to the Web version of this article.)

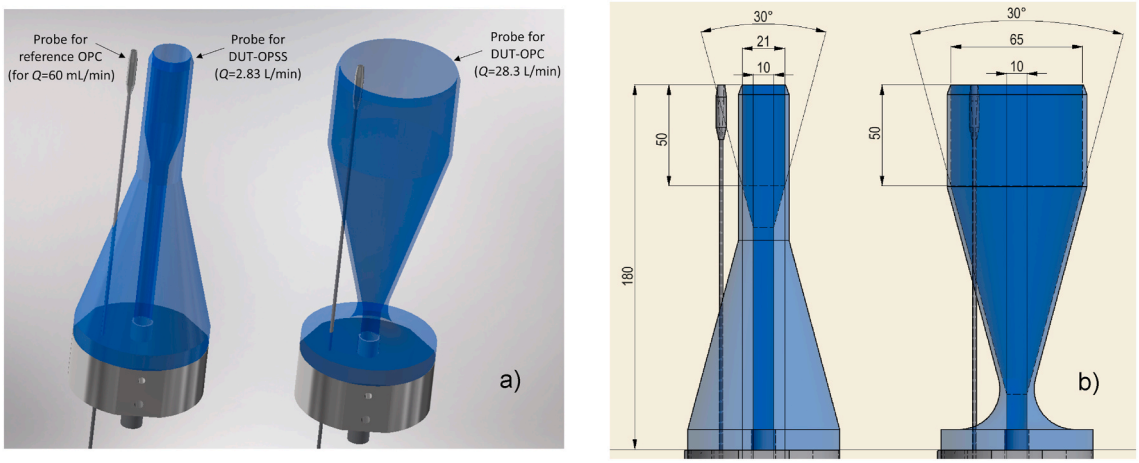

Fig. 3. a) and b) Computer-aided design (CAD, Inventor Professional 2019, Autodesk, USA) of the isokinetic sampling probes for the reference OPC and DUT. DUT stands for device under test. All isokinetic sampling probes are made of aluminium. The isokinetic sampling probes for the DUT are illustrated with a different colour (blue) for visualisation purposes only. The outer surface of the DUT sampling probe is depicted as transparent to reveal the inner design of the aerosol sampling pipe, but in reality it is made of solid aluminium. The dimensions in panel b) are given in mm. Note that the sampling probe for the reference OPC penetrates through the cone of the sampling probe for the DUT-OPC. (For interpretation of the references to colour in this figure legend, the reader is referred to the Web version of this article.)

2.2. Validation of the METAS primary standard at 10 μm

According to a previous inter-comparison in the size range 500 nm to 5 μm (Vasilatou et al., 2020), the primary standard at METAS (Fig. 1) and the primary standard at AIST (Japan) which is based on an inkjet aerosol generator IAG (Iida & Sakurai, 2018; Iida et al., 2014) exhibit good agreement in the measurement of particle number concentration (typically within 5%). For the purpose of this study, an additional inter-comparison was performed at 10 μm (PS optical diameter) to investigate the degree of equivalence of the two primary standards at sizes larger than 5 μm. A KC-31 OPC (Rion, Japan) was used as transfer standard and the experiments were carried out as described in (Vasilatou et al., 2020). During data evaluation at METAS and AIST, the particle counts of the DUT were integrated over a similar size-channel range to ensure measurement comparability. The results, summarised in Table 1, agree within the stated uncertainties. The counting efficiency of the transfer standard might have shifted by 0.01–0.02 during the transport process, which is not reflected in our uncertainty calculation. The inter-comparison was performed at low particle number concentrations since the IAG is best suited for generating aerosol concentrations below 1 cm^{-3}. The number concentration generated at METAS and AIST was 2.56 ± 0.16 cm^{-3} and 0.0654 ± 0.0004 cm^{-3}, respectively. The mismatch in concentration does not introduce any artefacts since the concentrations tested stay below the coincidence threshold (≤10% coincidence losses at 28 cm^{-3}) of the KC-31 OPC transfer standard.

2.3. Commercial optical particle size spectrometers used in this study

Two different commercially available OPSS were used in this study: the so-called Optical Particle Sizer (OPS) Model 3330 (TSI Inc., USA) and the Dust Monitor 11-D (Grimm GmbH, Germany).

The Model 3330 OPS is a light, portable spectrometer that provides fast measurement of particle number concentration and particle size distribution based on single-particle counting technology. The OPS has an inlet flow rate of 1 L/min and measures particles from 0.3 μm to 10 μm in 16 user-adjustable size channels. The instrument is battery powered for up to 20 h and is used in a wide variety of applications, ranging from filter testing to industrial/occupational measurements (Bush et al., 2014; Din et al., 2020), as well as both indoor (Maragkidou et al., 2018) and outdoor monitoring.

The Grimm 11-D monitor is a compact and portable instrument which measures particle number concentration and particle size distribution as well as PM (particulate matter) mass concentration (e.g. PM_{10}, PM_4, $PM_{2.5}$ and PM_1). The Grimm 11-D has an inlet flow rate of 1.2 L/min and measures particles from 0.253 μm to 35.15 μm in 31 predefined size channels. The instrument finds a wide range of applications in the field of aerosol research (Masic et al., 2020) and indoor air quality monitoring, e. g. at workplaces, interior of

Table 1
Counting efficiencies, *CE*, of the KC-31 OPC as determined by METAS and AIST. *U* designates expanded uncertainties (coverage factor $k = 2$; 95% confidence level).

Nominal particle size (μm)	*CE* measured by METAS $CE_{METAS} \pm U$	*CE* measured by AIST $CE_{AIST} \pm U$
10	1.012 ± 0.073	0.924 ± 0.056

vehicles, or for process analysis.

The concentration range of the TSI Model 3330 OPS and Grimm 11-D monitor is 0–3000 cm^{-3} and 0-5300 cm^{-3}, respectively. Above this upper concentration threshold, coincidence losses start to become significant and a dilution unit must be placed upstream of the OPSS.

3. Results and discussion

The setup described in Section 2.1 was used to calibrate four different Model 3330 OPS and two different 11-D units in the size range 300 nm to 10 μm. The results are summarised in Tables 2 and 3 and discussed in detail in Sections 3.1 and 3.2, respectively. The PS diameter, *d*, was either taken from calibration certificate of the PS particles provided by the manufacturer or determined at METAS in a traceable manner with atomic force microscopy (AFM). The counting efficiency of the DUT, CE_{DUT}, was calculated as $CE_{DUT} = C_{DUT}/C_{ref}$, where C_{DUT} and C_{ref} are the number concentrations measured by the DUT and the reference OPC, respectively. The value of CE_{DUT} is the arithmetic mean of at least 20 measurements, each measurement having a duration of 60 s. More details on the calculation of the counting efficiency are provided in section S2 of the Supporting Information. *U* denotes expanded uncertainties (coverage factor $k = 2$; 95% confidence level).

3.1. Calibration of TSI Model 3330 OPS

The calibration of the four different Model 3330 OPS units was performed at a nominal size of 300 nm, 500 nm, 1 μm, 5 μm and 10 μm. Since the ISO 21501-1 standard does not define which size bins of the DUT should be taken into account when evaluating the counting efficiencies and no consensus exists within the aerosol community, the size range of the DUT was selected based on different approaches (i.e. size range according to ISO 21501-4 or extended size range) as shown in Table 2. Note that the value of C_{DUT} (and thus *CE*) may depend on the size bins of the DUT which were taken into account during data analysis as will be discussed in Subsection 3.3.

The measurements were performed at different particle number concentrations, C_{ref}, with concentrations being as high as ~800 cm^{-3} at $d = 300$ nm, decreasing gradually to only a few particles per cm^{-3} at 10 μm. This trend simulates reasonably well ambient particle number concentrations which decrease as the particle size increases. It must be noted, however, that in urban environments during pollution events the particle number concentration at particle sizes below about 500 nm can reach several thousand or even tens of thousands particles per cm^{-3}. With the primary standard at METAS (Section 2.1), concentrations only up to 2000 cm^{-3} can be generated due to the high dilution factor of about 180 in the homogenizer (Horender et al., 2019).

Table 2
Calibration of four different Model 3330 OPS units (TSI inc., USA) with PS particles in the size range 300 nm to 10 μm. *d* is the certified average size of the PS calibration particles, $C_{ref,i}$ is the particle number concentration reported by the reference optical counter and $CE_{DUT,i}$ is the counting efficiency of the DUT. The index i (= 1 − 4) designates the number of the DUT-OPSS unit. *U* denotes expanded uncertainties (coverage factor $k = 2$; 95% confidence level).

$d \pm U$ (μm)	*Size Range of* $DUT_{1,2}$ (μm)	$C_{ref,\,1}$ (cm^{-3})	$CE_{DUT,\,1} \pm U$	$C_{ref,\,2}$ (cm^{-3})	$CE_{DUT,\,2} \pm U$
0.300 ± 0.010	0.30–0.50	746	0.961 ± 0.016	778	0.931 ± 0.015
0.497 ± 0.007	0.30–0.50 & 0.50–1.00	262	1.027 ± 0.017	263	0.997 ± 0.017
1.015 ± 0.030	0.50–1.00 & 1.00–5.00	23.5	1.000 ± 0.022	41.8	1.057 ± 0.018
4.980 ± 0.150	1.00–5.00 & 5.00–10.00	1.59	0.956 ± 0.041	1.52	0.967 ± 0.045
10.020 ± 0.120	5.00–10.00 & 10.00 - >10.00[b]	2.13	1.033 ± 0.042	2.49	0.996 ± 0.045

$d \pm U$ (μm)	*Size Range of* DUT_3 (μm)[a]	$C_{ref,\,3}$ (cm^{-3})	$CE_{DUT,\,3} \pm U$	$d \pm U$ (nm)	*Size Range of* DUT_4 (μm)	$C_{ref,\,4}$ (cm^{-3})	$CE_{DUT,\,4} \pm U$
0.305 ± 0.009	0.30–0.35 & 0.35–0.40	720	0.903 ± 0.015	0.302 ± 0.008	0.30–10.00	106	0.626 ± 0.010
0.512 ± 0.013	0.30–0.35 & 0.35–0.40 & 0.40–0.50 & 0.50–0.60 & 0.60-0.70	254	0.968 ± 0.017	0.503 ± 0.013	0.40–10.00	84.7	1.013 ± 0.018
1.015 ± 0.030	0.70–0.80 & 0.80–1.00 & 1.00–1.50	9.01	0.861 ± 0.020	1.005 ± 0.023	0.70–10.00	45.5	1.008 ± 0.018
4.980 ± 0.150	3.00–4.00 & 4.00–5.00 & 5.00–6.00 & 6.00–8.00	0.99	0.94 ± 0.07	5.067 ± 0.044	3.00–10.00	19.4	0.84 ± 0.07
10.020 ± 0.120	8.00–10.00 & 10.00 - >10.00[b]	1.32	1.02 ± 0.07	-[c]	-[c]	-[c]	-[c]

[a] Size range compatible with the ISO 21501-4 standard which defines an upper limit for the size resolution $R \leq 0.15$. See Subsection 3.3 for a more detailed discussion.

[b] The upper limit of the 10 μm size channel is not defined.

[c] The measurement at 10 μm was not performed due to limited availability of the instrument.

Table 3
Calibration of two different 11-D dust monitors (Grimm, Germany) with PS particles in the size range 300 nm to 10 μm. d is the certified average size of the PS calibration particles. $C_{ref,i}$ is the particle number concentration reported by the reference optical counter and $CE_{DUT,i}$ is the counting efficiency of the DUT. The index i (= 1 − 2) designates the number of the DUT 11-D unit. U denotes expanded uncertainties (coverage factor $k = 2$; 95% confidence level).

$d \pm U$ (μm)	*Size Range of DUT* (μm)	$C_{ref,\ 1}$ (cm^{-3})	$CE_{DUT,\ 1} \pm U$	$C_{ref,\ 2}$ (cm^{-3})	$CE_{DUT,\ 2} \pm U$
0.300 ± 0.010	≥0.253	614	0.982 ± 0.016	798	0.994 ± 0.016
0.497 ± 0.007	≥0.298	264	0.995 ± 0.017	311	1.004 ± 0.017
1.015 ± 0.030	≥0.488	21.9	0.918 ± 0.021	32.2	0.994 ± 0.018
1.998 ± 0.050	≥0.943	1.02	0.96 ± 0.06	3.31	0.976 ± 0.031
3.034 ± 0.060	≥0.943	1.00	0.880 ± 0.052	1.24	0.871 ± 0.044
4.980 ± 0.150	≥0.943	1.29	0.907 ± 0.046	1.32	0.909 ± 0.055
10.020 ± 0.120	≥4.884	1.03	0.854 ± 0.058	1.54	0.896 ± 0.049

The results are summarised in Table 2 and displayed graphically in Fig. 4 a). It can be seen that the Model 3330 OPS investigated in this study exhibit counting efficiencies well above 90% over the whole particle size range. The only exceptions are the *CE* of DUT 3 at 1 μm ($CE = 0.861$) and that of DUT 4 at 300 nm and 5 μm with $CE = 0.626$ and 0.84, respectively. It is worth noting that no decrease in *CE* due to impaction losses was observed at 5 μm and 10 μm. The results are not surprising. Units 1 and 2, which came directly from factory, exhibit an almost ideal behaviour. Similarly, unit 3, which underwent maintenance/service within a year from the calibration date at METAS shows high counting efficiencies while unit 4 which had not undergone service for more than 1 year exhibits a poorer counting efficiency. These results highlight the need for an annual maintenance check and recalibration by the manufacturer or other accredited laboratories.

While the Model 3330 TSI OPS starts measuring at 0.3 μm it seems to perform better than stated (can detect particles with size smaller than 0.3 μm). According to Section 3.2.2 of the ISO 21501-1 (see also Section 6.2 of ISO 21501-4), the lower size limit for particle size is defined by convention to be the smallest diameter at which the counting efficiency is 0.5 ± 0.15 (50% ± 15%; lower size limit of the measuring range). Assuming that the size distribution of the 300 nm PS particles is symmetric, the Model 3330 OPS having a lowest size threshold at 300 nm should measure only the upper half of the particle size distribution ($d \geq 300$ nm) and exhibit a *CE* of 50%. A *CE* of 90% implies that the "300 nm size threshold" is not so accurately adjusted and the lower limit corresponds to particle diameters smaller than 300 nm. In order to be better compliant with ISO 21501-1 and ISO 21501-4, it would be advisable that the manufacturer adds a new lower size limit to the Model 3330 OPS measuring range where the counting efficiency is only 50%.

Furthermore, in Section 3.2.3 of the ISO 21501-1 standard the upper size limit for the particle size is defined by convention to be the largest diameter at which the counting efficiency is 0,5 ± 0,15 (50% ± 15%; upper size limit of measuring range). In other words, an end-user of the Model 3330 OPS might mistakenly assume that the counting efficiency in the 10 μm size bin is 50% whereas, in reality, it is ~100%. To avoid such misunderstandings and achieve better compliance with the ISO 21501-1 and 21501-4 standards, it is recommended that the manufacturers define a new size bin above 10 μm for which $CE \approx 50\%$.

3.2. Calibration of Grimm 11-D monitor

The calibration of the two different 11-D monitors was performed at a nominal size of 300 nm, 500 nm, 1 μm, 2 μm, 3 μm, 5 μm and 10 μm. Both units had undergone maintenance within a year from the calibration date at METAS. As mentioned in Section 3.1, the ISO 21501-1 standard does not define which size bins of the DUT should be taken into account when evaluating the counting efficiencies. The size range can therefore be selected by the end-users and the calibration laboratory. For this set of experiments, the selected size range is listed in the second column of Table 3.

The measurements were performed at similar number concentrations as in the case of the Model 3330 OPS, i.e. the concentration

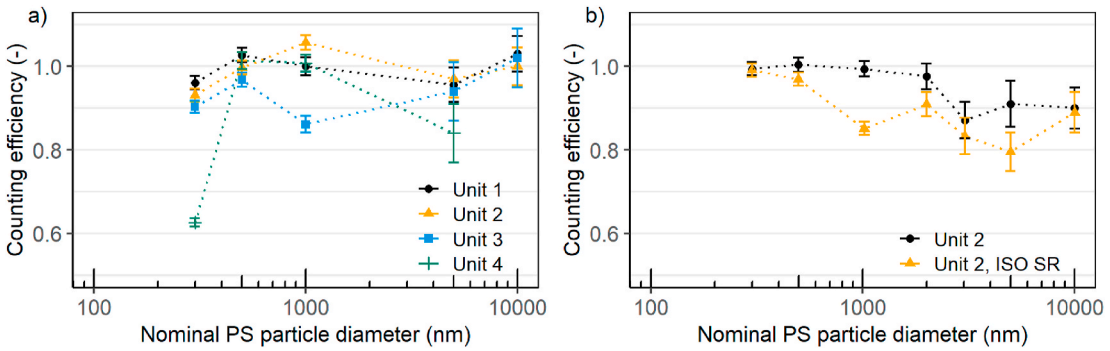

Fig. 4. Counting efficiency profile of a) four different TSI Model 3330 OPS units and b) the Grimm 11-D unit 2, with the particle counts integrated over different size ranges (see text for more details). "ISO SR" stands for size range according to ISO 21501-4. The error bars designate expanded measurement uncertainties (95% confidence level).

decreased gradually from about 700 cm^{-3} at 300 nm to a couple of particles per cm^{-3} at 10 μm. The counting efficiency of the two 11-D units is summarised in the 4th and 6th columns of Table 3. It can be seen that the two 11-D monitors investigated in this study exhibit high counting efficiencies up to 2 μm. At larger particle sizes a slight decrease is observed but the monitors still perform well with $CE \geq$ 85%.

The counting efficiency of the 11-D monitor at 300 nm is close to 100% as in the case of the Model 3330 OPS. The 11-D monitor, however, already possesses a lower size bin ranging from 0.25 to 0.30 μm. Unfortunately, due to the lack of certified particle standards at 250 nm we could not determine whether the counting efficiency at 250 nm would be 50% as required by the ISO standards 21501-1 and 21501-4.

3.3. Effect of the integrated size range on counting efficiency

No upper limit for the size resolution R is defined in the ISO 21501-1 (ISO 21501-1, 2009). The analysis presented in this section is based on the ISO 21501-4 (ISO 21501-4, 2018) which is dedicated to OPC for clean-room applications.

In the ISO 21501-4 standard, the size resolution is defined as

$$R = \frac{\sqrt{\sigma^2 - \sigma_c^2}}{d} \tag{1}$$

where

R: is the size resolution;

σ: is the apparent standard deviation of the size distribution of the calibration particles observed by the OPSS;

σ_c: is the standard deviation of the size distribution of the calibration particles;

d: is the certified average size of the calibration particles (in the ISO standard the symbol x_c is used).

In addition, according to Section 6.3 of the ISO 21501-4 the "size resolution must be less than or equal to 0,15 (corresponding to 15% of the specified particle size)" (ISO 21501-4, 2018). By setting $R = 0.15$ in Equation (1) and typing in the values of d and σ_c (determined at METAS by AFM or provided by the PS manufacturer), the maximum permissible σ of the OPSS can be calculated as shown in Table 4. Based on the calculation of σ_{max}, the OPSS size range where at least 95% of the PS particle counts are expected, $d + 2\,\sigma_{max}$, can be determined.

The counting efficiency profile of both 11-D units (Table 3) were recalculated by setting the size range equal to $\approx d \pm 2\sigma_{max}$. The results are listed in Table 5. The data evaluation of the third Model 3330 OPS unit (DUT 3 in Table 2) is already compatible with ISO 21501-4 to a good approximation. Note that the size channels of the 11-D monitor are not adjustable while those of the Model 3330 OPS are user adjustable but with certain limitations regarding channel width. Whenever it was not possible to set the upper or lower size threshold according to ISO 21501-4, the best possible approximation was made. In Table 2, it can be seen that the *CE* profile of the Model 3330 OPS unit 3 is comparable to those of units 1 and 2 except for the measurement at 1 μm where the *CE* drops to 0.861. By inspecting the output data file of the instrument, we found out that this observation is not related to the narrower selection of the size channels (in an extended size range between 0.5 μm and 2.5 μm, *CE* would only increase by 1–2%).

However, the *CE* of both 11-D units decreases by as much as 10% at particle sizes 1 μm and 5 μm as summarised in Table 5 and shown graphically in Fig. 4 for unit 2. To investigate the reason of this discrepancy, we examined the output data file of the 11-D units. In Fig. 5, the particle counts per size channel of 11-D unit 2 are displayed in the case of the a) 5 μm PS particles and b) 1 μm PS particles. In Fig. 5 a), the peak at around 300 nm is due to residue particles and must be neglected. Apart from the main peak at around 5 μm (particle counts in the size channels 4.14–4.88 and 4.88–5.76) which is due to PS particles, a front tail is observed between 2.5 μm and 4 μm. One possible explanation is that these counts arise from PS particles which cross the laser beam at the edge, scattering less light and thus being classified as smaller particles. In Table 2, by summing all particle counts at sizes ≥0.943 μm (black dashed line in Fig. 5a) the front tail is treated as extension of the main peak and the counts between 2.5 μm and 4 μm contribute to the counting efficiency of the DUT. In Table 5, however, only the counts in the size channels 3.52–6.79 μm (denoted by the green and red dashed

Table 4
Certified average size of the calibration particles, d, standard deviation of the size distribution of the calibration particles, σ_c, maximum permissible standard deviation of the size distribution of the calibration particles, σ_{max}, and size range according to ISO 21501-4.

$d \pm U$ (μm)	$2\sigma_c$ [a] (μm)	$2\sigma_{max}$ (μm) [b]	$d\text{-}2\sigma_{max} - d+2\sigma_{max}$ (μm) [Size Range ISO 21501-4] [b]
0.300 ± 0.010	0.010	0.091	0.209–0.391
0.497 ± 0.007	0.007	0.149	0.348–0.646
1.015 ± 0.030	0.019	0.305	0.710–1.320
1.998 ± 0.050	0.050	0.601	1.397–2.599
3.034 ± 0.060	0.060	0.912	2.122–3.946
4.980 ± 0.150	0.150	1.502	3.478–6.482
10.020 ± 0.120	0.110	3.008	7.012–13.028

[a] Referred to simply as standard deviation (instead of expanded standard deviation) on the calibration certificates provided by the PS manufacturers. However, according to personal communication with PS providers the standard deviation on the certificates is given for a coverage factor $k = 2$ (95% confidence level), hence in Table 4 we use the symbol $2\sigma_c$.

[b] Calculated by setting $R = 0.15$ in Equation (1).

Table 5
Calibration of two different 11-D dust monitors (Grimm, Germany) with PS particles in the size range 300 nm to 10 μm. d is the certified average size of the PS calibration particles. $C_{ref,i}$ is the particle number concentration reported by the reference optical counter and $CE_{DUT,i}$ is the counting efficiency of the DUT. The index i (= 1 − 2) designates the number of the DUT 11-D unit. U denotes expanded uncertainties (coverage factor $k = 2$; 95% confidence level). The size range has been defined according to the ISO 21501-4 standard.

$d \pm U$ (μm)	*Size Range of DUT** (μm)	$C_{ref,\ 1}$ (cm^{-3})	$CE_{DUT,\ 1} \pm U$	$C_{ref,\ 2}$ (cm^{-3})	$CE_{DUT,\ 2} \pm U$
0.300 ± 0.010	0.25–0.30 & 0.30–0.35 & 0.35–0.41	614	0.980 ± 0.016	798	0.991 ± 0.016
0.497 ± 0.007	0.35–0.41 & 0.41–0.49 & 0.49–0.58 & 0.58–0.68	264	0.979 ± 0.017	311	0.969 ± 0.016
1.015 ± 0.030	0.68–0.80 & 0.80–0.94 & 0.94–1.11 & 1.11–1.31	21.9	0.831 ± 0.019	32.2	0.851 ± 0.016
1.998 ± 0.050	1.31–1.55 & 1.55–1.82 & 1.81–2.15 & 2.15–2.53	1.02	0.892 ± 0.056	3.31	0.909 ± 0.029
3.034 ± 0.060	2.15–2.53 & 2.53–2.98 & 2.98–3.52 & 3.52–4.14	1.00	0.840 ± 0.050	1.24	0.833 ± 0.044
4.980 ± 0.150	3.52–4.14 & 4.14–4.88 & 4.88–5.76 & 5.76–6.79	1.29	0.798 ± 0.039	1.32	0.795 ± 0.046
10.020 ± 0.120	6.79–8.00 & 8.00–9.43 & 9.43–11.12 & 11.12–13.10	1.03	0.825 ± 0.056	1.54	0.890 ± 0.048

lines in Fig. 5a) are taken into account and as a result *CE* drops by about 10%.

In the case of the 1 μm PS particles, a tail towards larger particle sizes is observed as shown in Fig. 5b). By integrating only the particle counts in the size range 0.68–1.31 μm (green and red dashed lines in Fig. 5b)) according to ISO 21501-4 (see Table 5), the counts in the range 1.31–2.15 μm are not taken into account and the counting efficiency drops by about 14% as shown in Fig. 4b). A possible explanation for this observation might be the non-monotonic nature of the scattered light intensity as a function of the particle diameter at around 1–1.5 μm (Walser, Sauer, Spanu, Gasteiger, & Weinzierl, 2017).

From these examples it becomes clear that the size range of the DUT considered during the data analysis can have a considerable impact on the determination of the counting efficiency. Currently, the ISO 21501-1 standard sets no upper limit for the size resolution of the instruments nor does it make any recommendations on how to evaluate the counting efficiency. This lack of standardised procedures creates confusion among OPSS end-users and calibration laboratories and may lead to significant calibration biases. We would recommend that the ISO 21501-1 standard be revised in order to define i) a detailed procedure for the determination of the OPSS counting efficiency and ii) an upper limit for the OPSS size resolution as a function of particle size for calibration of the counting efficiency. The data presented in this study suggest that the upper limit of the size resolution might need to be extended beyond 15% at certain particle sizes. We hope that the work reported in this study can serve as input towards a better standardisation of OPSS.

4. Conclusions

In this study, we present a traceable method for determining the counting efficiency of optical particle size spectrometers (OPSS). The primary standard consists of an aerosol generation setup, a vertical flow tube for particle homogenization and a reference optical particle counter (OPC). The OPSS under testing and the reference optical particle counter sample aerosol simultaneously through specially designed isokinetic sampling probes. Calibration in terms of particle size relies by convention on the use of certified PS (polystyrene) spheres in the size range 100 nm - 10 μm. The method can be applied in a wide number concentration range from 0.5 cm^{-3} up to about 2000 cm^{-3} (depending on the particle size).

Four different Model 3330 OPS (TSI Inc., USA) units and two different 11-D monitors (Grimm GmbH, Germany) were calibrated against the primary standard and the counting efficiency *CE* was calculated. The relative expanded uncertainty (95% confidence level) in the determination of CE_{DUT} varied between 2% at number concentrations >30 cm^{-3} to 7% at concentrations <2 cm^{-3}.

Three of the Model 3330 OPS units exhibited high counting efficiencies (>85%) over the whole size range of the instrument (300 nm − 10 μm). The fourth unit of Model 3330 OPS, which is due for recalibration by the manufacturer, showed a much lower *CE* of about 60% at 300 nm.

The counting efficiency profile of the 11-D monitors depended on the size range considered during data analysis. *CE* remained close

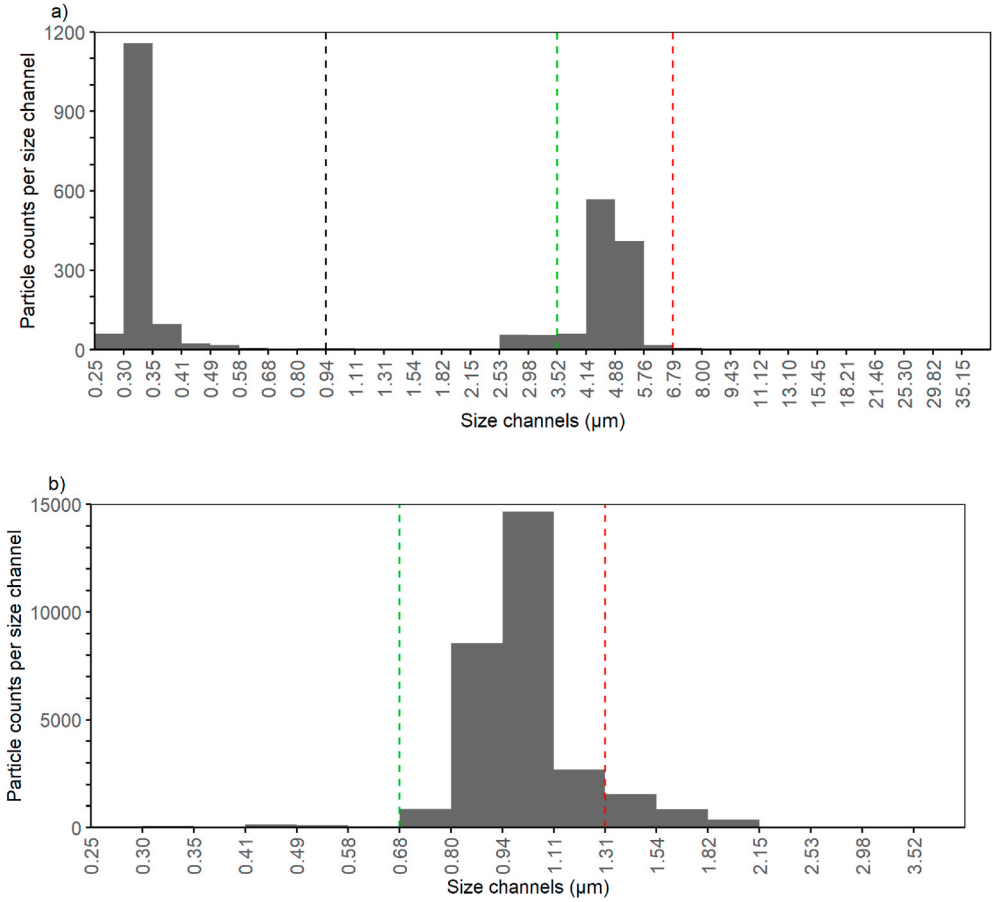

Fig. 5. Particle counts per size channel reported by the second 11-D unit in the case of a) 5 μm PS particles and b) 1 μm PS particles. The green and red dashed lines denote the upper and lower size thresholds to be considered during data analysis according to the ISO 21501-4 standard (Table 4). (For interpretation of the references to colour in this figure legend, the reader is referred to the Web version of this article.)

to or exceeded 90% when the particle counts were integrated over a sufficiently large size range. However, at 1 μm and 5 μm the *CE* dropped by about 10% when a narrower size range, e.g. according to the ISO 21501–4:2018 standard on OPC for clean rooms, was applied.

The ISO 21501-1 standard on the calibration of OPSS does not set an upper limit for the size resolution nor does it define the size range to be taken into account during calculation of the counting efficiency. This lack of clear guidelines causes confusion among aerosol scientists and calibration laboratories and may lead to measurement biases. We recommend that the ISO 21501-1 standard be revised to provide a more detailed procedure for the determination of the OPSS counting efficiency and an upper limit for the OPSS size resolution as a function of particle size for calibration of the counting efficiency.

Funding

Part of the work carried out by METAS and DTI has been funded by the 19ENV08 Aeromet II project of the European Union through the European Metrology Programme for Innovation and Research (EMPIR). EMPIR is jointly funded by the EMPIR participating countries within EURAMET and the European Union. METAS was also supported by internal funds.

Data availability

The OPSS data that support the findings of this study will become openly available once the manuscript has been accepted for publication.

Declaration of competing interest

The authors declare that they have no known competing financial interests or personal relationships that could have appeared to

influence the work reported in this paper.

Acknowledgement

We would like to thank Sensirion AG (Switzerland) for providing us with one of the Model 3330 OPS units.

Appendix A. Supplementary data

Supplementary data to this article can be found online at https://doi.org/10.1016/j.jaerosci.2021.105818.

References

Alas, H. D. C., Weinhold, K., Costabile, F., Di Ianni, A., Müller, T., Pfeifer, S., et al. (2019). Methodology for high-quality mobile measurement with focus on black carbon and particle mass concentrations. *Atmospheric Measurement Techniques, 12*, 4697–4712. https://doi.org/10.5194/amt-12-4697-2019

Bezantakos, S., Schmidt-Ott, F., & Biskos, G. (2018). Performance evaluation of the cost-effective and lightweight Alphasense optical particle counter for use onboard unmanned aerial vehicles. *Aerosol Science and Technology, 52*, 385–392. https://doi.org/10.1080/02786826.2017.1412394

Bush, K. J., Heflin, K. R., Marek, G. W., Bryant, T. C., & Auvermann, B. W. (2014). Increasing stocking density reduces emissions of fugitive dust from cattle feedyards. *Applied Engineering in Agriculture, 30*(5), 815–824. https://doi.org/10.13031/aea.30.10681

Chen, B. T., Cheng, Y. S., & Yeh, H. C. (1984). Experimental responses of two optical particle counters. *Journal of Aerosol Science, 15*, 457–464. https://doi.org/10.1016/0021-8502(84)90041-7

Deshler, T., Hervig, M. E., Hofmann, D. J., Rosen, J. M., & Liley, J. B. (2003). Thirty years of in situ stratospheric aerosol size distribution measurements from Laramie , Wyoming (41 ° N), using balloon-borne instruments. *Journal of Geophysical Research, 108*, 4167. https://doi.org/10.1029/2002JD002514

Din, A. R., Hindocha, A., Patel, T., Sudarshan, S., Cagney, N., Koched, A., et al. (2020). Quantitative analysis of particulate matter release during orthodontic procedures: A pilot study. *British Dental Journal*. https://doi.org/10.1038/s41415-020-2280-5, 1–7.

Hermann, M., Weigelt, A., Assmann, D., Pfeifer, S., Müller, T., Conrath, T., et al. (2016). An optical particle size spectrometer for aircraft-borne measurements in IAGOS-CARIBIC. *Atmospheric Measurement Techniques, 9*, 2179–2194. https://doi.org/10.5194/amt-9-2179-2016

Högström, R., Quincey, P., Sarantaridis, D., Lüönd, F., Nowak, A., Riccobono, F., et al. (2014). First comprehensive inter-comparison of aerosol electrometers for particle sizes up to 200 nm and concentration range 1000 cm-3 to 17000 cm-3. *Metrologia, 48*, 426–436. https://doi.org/10.1088/0026-1394/51/3/293

Horender, S., Auderset, K., & Vasilatou, K. (2019). Facility for calibration of optical and condensation particle counters based on a turbulent aerosol mixing tube and a reference optical particle counter. *Review of Scientific Instruments, 90*, Article 075111. https://doi.org/10.1063/1.5095853

Iida, K., & Sakurai, H. (2018). Counting efficiency evaluation of optical particle counters in micrometer range by using an inkjet aerosol generator. *Aerosol Science and Technology, 52*(10), 1156–1166. https://doi.org/10.1080/02786826.2018.1505032

Iida, K., Sakurai, H., Saito, K., & Ehara, K. (2014). Inkjet aerosol generator as monodisperse particle number standard. *Aerosol Science and Technology, 28*(8), 789–802. https://doi.org/10.1080/02786826.2014.930948

ISO 21501-1. (2009). *ISO 21501-1:2009 Determination of particle size distribution – Single particle light interaction methods – Part 1: Light scattering particle spectrometer*.

ISO 21501-4. (2018). *ISO 21501-4:2018 Determination of particle size distribution – Single particle light interaction methods – Part 4: Light scattering airborne particle counter for clean spaces*.

ISO-27891. (2015). *ISO 27891:2015 Aerosol particle number concentration – Calibration of condensation particle counters*.

Järvinen, A., Keskinen, J., & Yli-Ojanperä, J. (2018). Extending the Faraday cup aerosol electrometer based calibration method up to 5 μm. *Aerosol Science and Technology, 52*(8), 828–840. https://doi.org/10.1080/02786826.2018.1472742

Johnson, T. J., Irwin, M., Symonds, J. P. R., Olfert, J. S., & Boies, A. M. (2018). Measuring aerosol size distributions with the aerodynamic aerosol classifier. *Aerosol Science and Technology, 52*(6), 655–665. https://doi.org/10.1080/02786826.2018.1440063

Kim, Y. J. (1995). Response of the active scattering aerosol spectrometer probe (ASASP-100X) to particles of different chemical composition. *Aerosol Science and Technology, 6826*(22), 33–42. https://doi.org/10.1080/02786829408959726

Krejci, R., Stro, J., Reus, M. De, Hoor, P., Williams, J., Fischer, H., et al. (2003). Evolution of aerosol properties over the rain forest in Surinam , South America , observed from aircraft during the LBA-CLAIRE 98 experiment. *Journal of Geophysical Research, 108*, 4561. https://doi.org/10.1029/2001JD001375

Kupc, A., Williamson, C., Wagner, N. L., Richardson, M., & Brock, C. A. (2018). Modification , calibration , and performance of the Ultra-High Sensitivity Aerosol Spectrometer for particle size distribution and volatility measurements during the Atmospheric Tomography Mission (ATom) airborne campaign. *Atmospheric Environment, 11*, 369–383. https://doi.org/10.5194/amt-11-369-2018

Liu, B. Y. H., Berglund, R. N., & Agarwal, J. K. (1974). Experimental studies of optical particle counters. *Atmospheric Environment, 8*, 717–732. https://doi.org/10.1016/0004-6981(74)90163-2

Mann, G. W., Carslaw, K. S., Reddington, C. L., Pringle, K. J., Schulz, M., Asmi, A., et al. (2014). Intercomparison and evaluation of global aerosol microphysical properties among AeroCom models of a range of complexity. *Atmospheric Chemistry and Physics, 14*, 4679–4713. https://doi.org/10.5194/acp-14-4679-2014

Maragkidou, A., Jaghbeir, O., Hämeri, K., & Hussein, T. (2018). Aerosol particles (0 . 3 – 10 μm) inside an educational workshop – Emission rate and inhaled deposited dose. *Building and Environment, 140*(May), 80–89. https://doi.org/10.1016/j.buildenv.2018.05.031

Masic, A., Bibic, D., Pikula, B., Blazevic, A., Huremovic, J., & Zero, S. (2020). Evaluation of optical particulate matter sensors under realistic conditions of strong and mild urban pollution. *Atmospheric Measurement Techniques, 13*, 6427–6443. https://doi.org/10.5194/amt-13-6427-2020

Ortega, J., Snider, J. R., Smith, J. N., & Reeves, J. M. (2019). Comparison of aerosol measurement systems during the 2016 airborne ARISTO campaign. *Aerosol Science and Technology, 53*(8), 871–885. https://doi.org/10.1080/02786826.2019.1610554

Owen, M., Mulholland, G., & Guthrie, W. (2012). Condensation particle counter proportionality calibration from 1 Particle·cm−3 to 10^4 Particles·cm−3. *Aerosol Science and Technology, 46*(4), 444–450. https://doi.org/10.1080/02786826.2011.637998

Renard, J.-B., Dulac, F., Berthet, G., Lurton, T., Vignelles, D., Jégou, F., et al. (2016). Loac: A small aerosol optical counter/sizer for ground-based and balloon measurements of the size distribution and nature of atmospheric particles – Part 1: Principle of measurements and instrument evaluation. *Atmospheric Measurement Techniques, 9*, 1721–1742. https://doi.org/10.5194/amt-9-1721-2016

Rosenberg, P. D., Dean, A. R., Williams, P. I., Dorsey, J. R., Minikin, A., Pickering, M. A., et al. (2012). Particle sizing calibration with refractive index correction for light scattering optical particle counters and impacts upon PCASP and CDP data collected during the Fennec campaign. *Atmospheric Measurement Techniques, 5*, 1147–1163. https://doi.org/10.5194/amt-5-1147-2012

Sang-Nourpour, N., & Olfert, J. S. (2019). Calibration of optical particle counters with an aerodynamic aerosol classifier. *Journal of Aerosol Science, 138*, 105452. https://doi.org/10.1016/j.jaerosci.2019.105452

Sauvageat, E., Zeder, Y., Auderset, K., Calpini, B., Clot, B., Crouzy, B., et al. (2020). Real-time pollen monitoring using digital holography. *Atmospheric Measurement Techniques, 13*, 1539–1550. https://doi.org/10.5194/amt-13-1539-2020

Sousan, S., Koehler, K., Hallett, L., & Peters, T. M. (2016). Evaluation of the Alphasense optical particle counter (OPC-N2) and the Grimm portable aerosol spectrometer (PAS-1.108). *Aerosol Science and Technology, 50*(12), 1352–1365. https://doi.org/10.1080/02786826.2016.1232859

Stolzenburg, M., Kreisberg, N., & Hering, S. (1998). Atmospheric size distributions measured by differential mobility optical particle size Spectrometry. *Aerosol Measurement: Principles, Techniques, and Applications, 29*(5), 402–418. https://doi.org/10.1080/02786829808965579

Tran, S., Iida, K., Yashiro, K., Murashima, Y., Sakurai, H., & Olfert, J. S. (2020). Determining the cutoff diameter and counting efficiency of optical particle counters with an aerodynamic aerosol classifier and an inkjet aerosol generator. *Aerosol Science and Technology, 54*(11), 1335–1344. https://doi.org/10.1080/02786826.2020.1777252

Vasilatou, K., Dirscherl, K., Iida, K., Sakurai, H., Horender, S., & Auderset, K. (2020). Calibration of optical particle counters: First comprehensive inter-comparison for particle sizes up to 5 μm and number concentrations up to 2 cm−3. *Metrologia, 57*(2), Article 025005. https://doi.org/10.1088/1681-7575/ab5c84

Walser, A., Sauer, D., Spanu, A., Gasteiger, J., & Weinzierl, B. (2017). On the parametrization of optical particle counter response including instrument-induced broadening of size spectra and a self-consistent evaluation of calibration measurements. *Atmospheric Measurement Techniques, 10*, 4341–4361. https://doi.org/10.5194/amt-10-4341-2017

Yli-Ojanperä, J., Sakurai, H., Iida, K., Mäkelä, J. M., Ehara, K., & Keskinen, J. (2012). Comparison of three particle number concentration calibration standards through calibration of a single CPC in a wide particle size range. *Aerosol Science and Technology, 46*(11), 1163–1173. https://doi.org/10.1080/02786826.2012.701023